Supporting Information

Saijo et al. 10.1073/pnas.1108810108

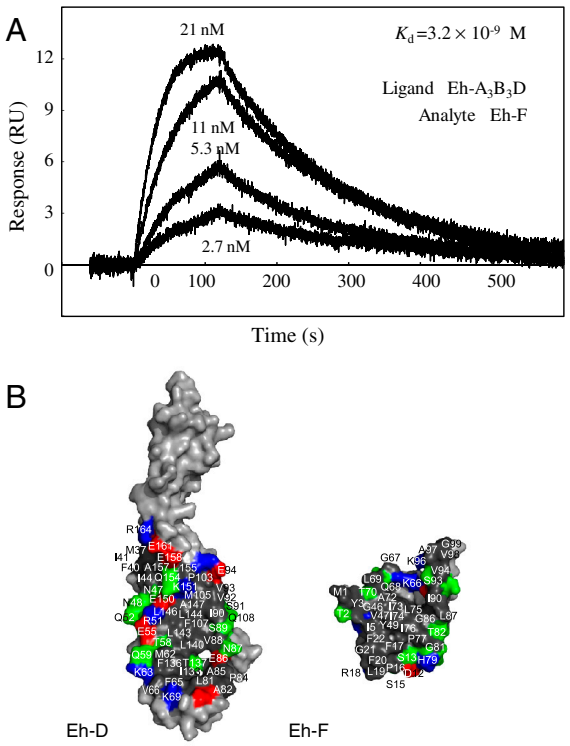

Fig. S1. Interactions between Eh-D and Eh-F. (*A*) Binding measurement was performed using the Biacore system. Sensorgrams for the binding of various concentrations of the analyte (Eh-F) to the ligand (Eh-A_3B_3D) are shown. (*B*) Surface representation of the interface between Eh-D and Eh-F: Polar residues (N, Q, S, T) are colored in green, positively charged residues (H, K, R) are blue, negatively charged residues (D, E) are red, and hydrophobic residues (A, C, F, G, L, M, P, V, W, Y) are dark gray. The residues with buried surface area of >10 Å^2 are mapped on the surface.

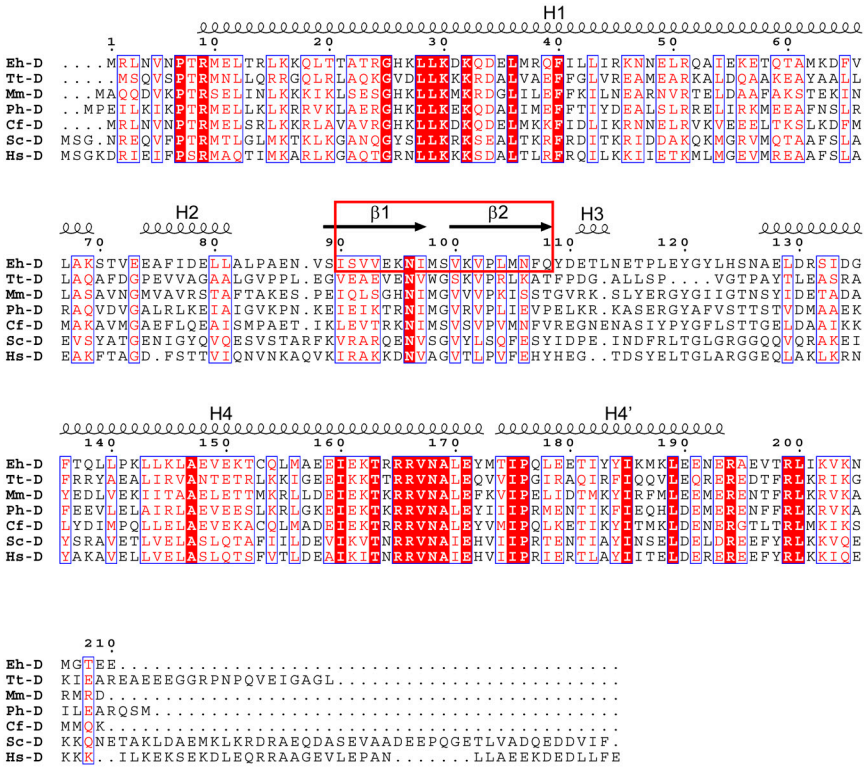

Fig. S2. Sequence alignment of the D subunits from different species. The primary sequences of the D subunits of V-ATPase were aligned: Eh-D, *Enterococcus hirae*; Tt-D; *Thermus thermophilus* HB8; Mm-D; *Methanosarcina mazei* Gö1; Ph-D, *Pyrococcus horikoshii*; Cf-D, *Clostridium fervidus*; Sc-D, *Saccharomyces cerevisiae*; and Hs-D, *Homo sapiens* . The secondary structures of Eh-D are shown above the sequences. The deleted region (90–108) of the mutation is indicated in the red box. The Dm mutant was constructed by the deletion of the β-hairpin region (90–108) and the insertion of two linker residues (GS).

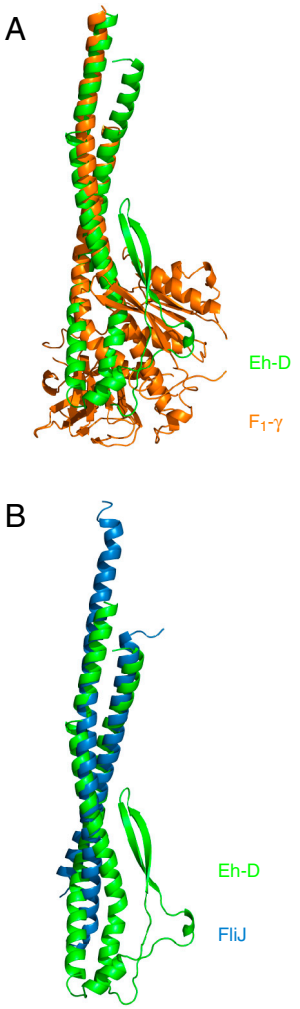

Fig. S3. Structural similarity of Eh-D with the γ-subunit and FliJ. (*A*) Eh-D (green) is superimposed with the γ-subunit (orange) of bovine F_1-ATPase [Protein Data Bank (PDB) ID 1E79]. (*B*) Eh-D (green) is superimposed with FliJ (light blue) of *Salmonella* flagellar type III protein export apparatus (PDB ID 3AJW).

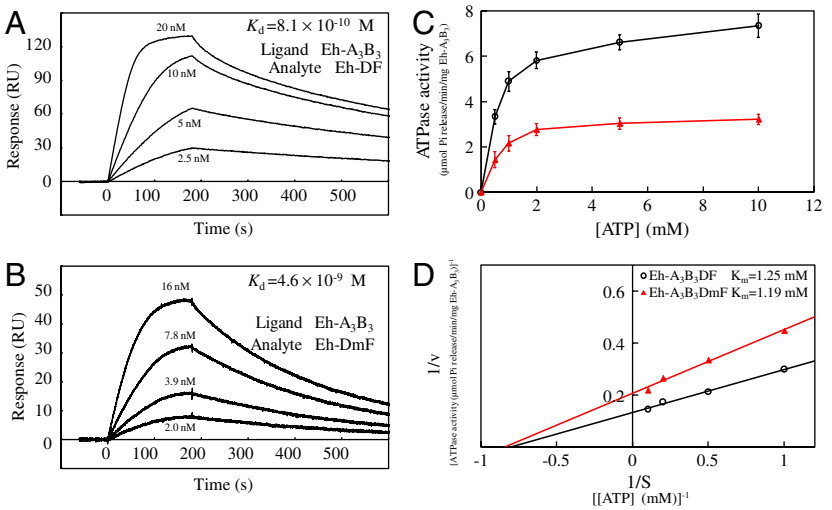

Fig. S4. Effect of the β-hairpin region of the D subunit. Binding measurements were performed using the Biacore system. Sensorgrams for the binding of various concentrations of analyte to ligand are shown. (*A*) Analyte, Eh-DF; ligand, Eh-A_3B_3. (*B*) Analyte, Eh-DmF; ligand, Eh-A_3B_3. (*C*) ATP concentration dependence of the ATPase activity of reconstituted Eh-A_3B_3DF (circle, black) and Eh-A_3B_3DmF (triangle, red). (*D*) The double reciprocal plot for the ATPase activity assay.

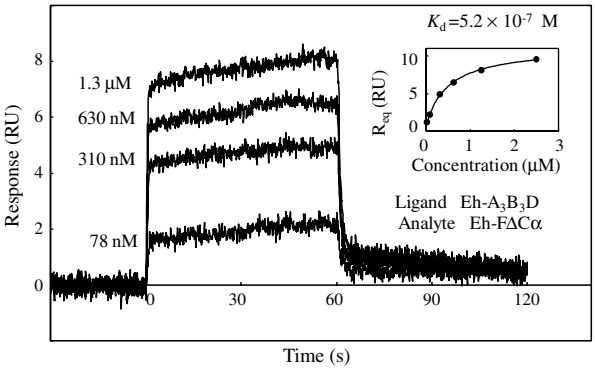

Fig. S5. Interactions between Eh-D and Eh-FΔCα. Binding measurements were performed using the Biacore system. Sensorgrams for the binding of various concentrations of the analyte (Eh-FΔCα) to the ligand (Eh-A_3B_3D) are shown. The inset shows the kinetic plot and binding isotherm for binding.

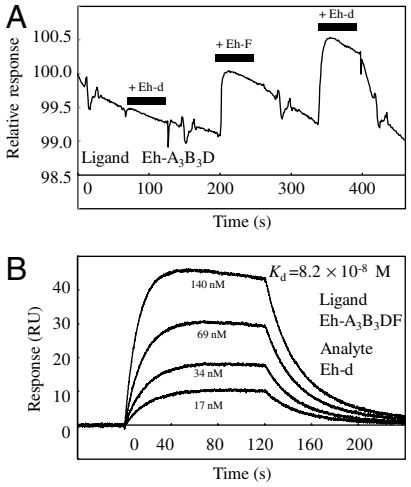

Fig. S6. Interaction of Eh-d. (*A*) Binding measurements were performed using the Biacore system. Sensorgram for the binding order of two analytes to the ligand is shown. After the immobilization of the ligand (Eh-A_3B_3D) onto the sensor chip, Eh-d and Eh-F were manually injected. Black bars indicate the injection period of each analyte. In the first injection of Eh-d, no specific binding response between Eh-A_3B_3D and Eh-d was observed. A specific binding response between Eh-A_3B_3D and Eh-F was observed in the injection of Eh-F. An additional binding response in the second injection of Eh-d corresponded to the interaction between Eh-A_3B_3DF and Eh-d. (*B*) Binding measurements were performed using the Biacore system. Sensorgrams for the binding of various concentrations of the analyte (Eh-d) to the ligand (Eh-A_3B_3DF) are shown.

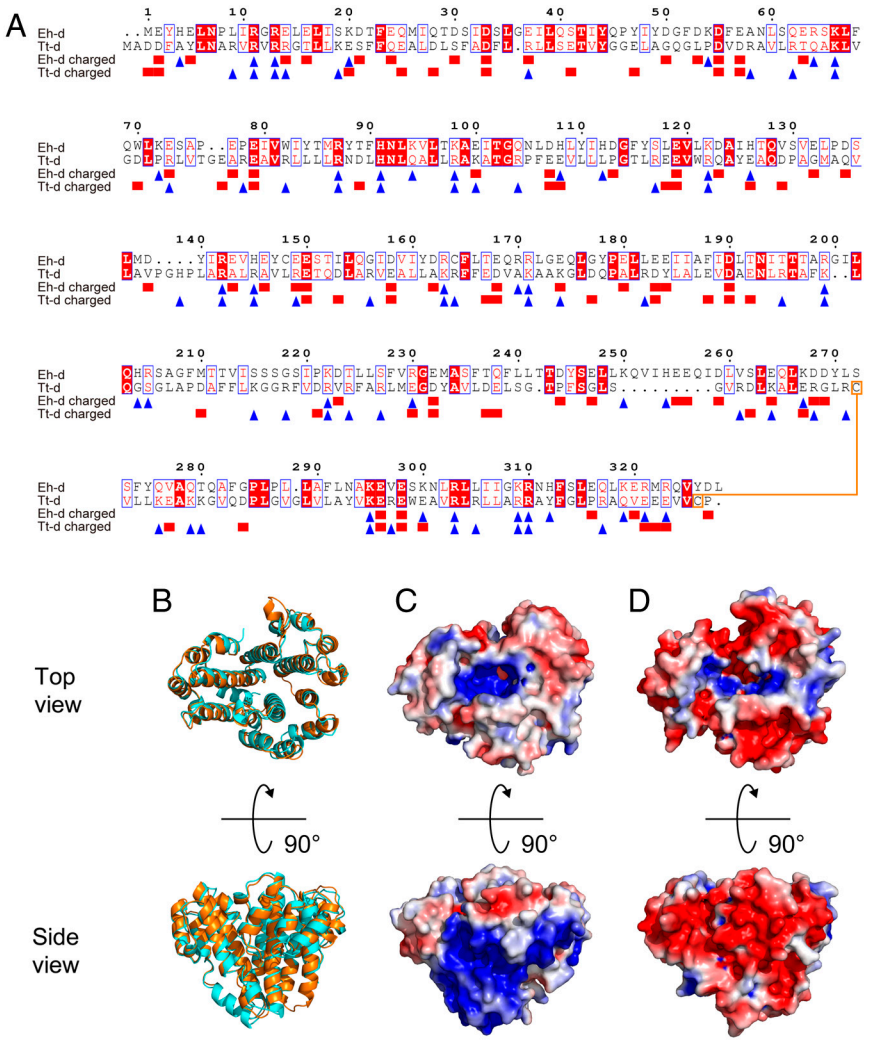

Fig. S7. Amino acid sequence similarity between Eh-d and Tt-d and homology modeling of Eh-d structure. (*A*) Sequence alignment of Eh-d and Tt-d. The charged residues are shown with red squares (positively charged) and blue triangles (negatively charged) below the sequence. The disulfide bonded cysteine residues are indicated with an orange box and line. (*B*) The homology model of Eh-d (orange) is superimposed with Tt-d (light blue). Electrostatic potential surface of Tt-d (*C*) and homology model of Eh-d (*D*) were produced in the same manner as in Fig. 5.

Table S1. Data collection and refinement statistics

	SeMet crystal*			
Data collection				
Space group		*C*2		
Cell dimensions				
a, *b*, *c*, Å		105.79, 68.43, 51.15		
α, β, γ, °		90, 114.99, 90		
	Peak (reprocessed)	*Peak*	*Inflection*	*Remote*
Wavelength, Å	0.9791	0.9791	0.9794	1.000
Resolution,† Å	2.00 (2.11-2.00)	2.10 (2.21-2.10)	2.10 (2.21-2.10)	2.10 (2.21-2.10)
R_{merge}†	0.090 (0.561)	0.084 (0.394)	0.048 (0.245)	0.045 (0.300)
$I/\sigma I$†	10.7 (2.8)	14.9 (3.8)	11.0 (3.0)	11.6 (2.9)
Completeness,† %	97.2 (96.3)	97.4 (96.4)	97.0 (96.0)	96.9 (95.9)
Redundancy†	6.1 (6.1)	6.1 (6.1)	2.0 (2.1)	2.0 (2.0)
Refinement				
Resolution,† Å	2.00 (2.05-2.00)			
No. reflections†	21,696 (1,503)			
R_{work}/R_{free}†	19.4(26.3)/25.2(29.0)			
No. atoms				
Protein	2,341			
Ligand/ion	4			
Water	152			
B factors				
Protein	41.8			
Ligand/ion	56.7			
Water	47.7			
rmsd				
Bond lengths, Å	0.011			
Bond angles, °	1.276			

*All datasets were obtained from one selenomethionine (SeMet)-labeled crystal.
†Values in parentheses are for the highest-resolution shell.